Inorganic Chemistry

Article

pubs.acs.org/IC

Solid-State Structural Studies of Chromium(III) Nicotinato Nutritional Supplements

T. H. Nguyen Pham,[†] Jade B. Aitken,[†,‡,§] Aviva Levina,[†] and Peter A. Lay*[,†]

[†]School of Chemistry, The University of Sydney, Sydney, New South Wales 2006, Australia

[‡]Australian Synchrotron, Clayton, Victoria 3168, Australia

[§]Institute of Materials Structure Science, KEK, Tsukuba, Ibaraki 305-0801, Japan

Supporting Information

ABSTRACT: While Cr(III) dietary supplements are widely consumed, some commercial supplements have yet to be structurally characterized. X-ray absorption spectroscopy and other spectroscopic methods were used to characterize Cr(III) nicotinato nutritional supplements that have long been used in complementary medicine. Different ratios of nicotinic acid and $CrCl_3 \cdot 6H_2O$ (*trans*-$[CrCl_2(OH_2)_4]Cl \cdot 2H_2O$) at different pH values gave a range of products. The local structures of Cr(III) nicotinato complexes obtained at pH 7 and of the patented complex were characterized by performing multiple-scattering analysis of their EXAFS spectra as well as EPR, UV−vis, and IR spectroscopies. For the first time, these complexes have been definitively characterized as nicotinato-bridged polymers of dihydroxido-bridged dinuclear Cr(III) cores. In the patented complex used in commercial preparations, each Cr is octahedral with an additional terminal O-bound nicotinato ligand, two bridging nicotinato (one O and one N bound), and an aqua ligand. The other species also have two or three bridging nicotinato ligands and an aqua and, in some cases, a terminal hydroxido ligand, which is dependent upon the stoichiometry of the reactants and the pH value of the solution in which they are prepared.

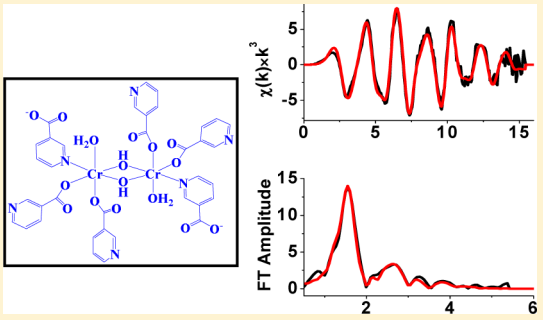

INTRODUCTION

Chromium(III) was originally postulated as an essential nutrient that played a role in carbohydrate and lipid metabolism.[1] Historically, Mertz and co-workers reported the isolation of a glucose tolerance factor (GTF) in which Cr(III) was proposed to be the active ingredient.[2,3] The absence of this GTF in the diet was believed to be responsible for the glucose intolerance in tested rats, but this postulate was subsequently shown to be incorrect.[4,5] Before experimental evidence was published that challenged the GTF hypothesis, this hypothesis spurred widespread interest in developing Cr(III) supplements, such as Cr(III) picolinato, Cr(III) nicotinato, Cr(III) citrato, and Cr(III) amino acids complexes. Despite this, their use as nutritional supplements for animals and humans as a proposed means of enhancing glucose metabolism, including weight loss, building muscles, and regulation of blood glucose levels in type 2 diabetes, has continued.[1,5] Indeed, the role of Cr(III) as an essential trace element is controversial since recent evidence has failed to replicate previous experiments that have pointed to it being essential and thrown doubt on the methodology of the original experiments.[6,7] Furthermore, the safety of Cr(III) supplements has also been questioned in light of a range of in vitro and in vivo experiments that point to a potential carcinogenicity of Cr(III).[7,8]

Because it was purported to be the component of GTF in 1981, a Cr(III) nicotinato complex was synthesized and marketed and gained substantial use as a nutritional supplement and is still sold.[9] Many studies on the chemical structures, biological activities, and toxicology of Cr(III) nicotinato complexes have been performed.[10−16] However, its structure and those of its metabolic pathways have not been elucidated. Hence, unlike other Cr(III) compounds used as nutritional supplements, Cr(III) nicotinato complexes are not well characterized. The synthetic procedures for Cr(III) nicotinato complexes that involve the use of Cr(III) chloride or Cr(III) nitrate, nicotinic acid (nicH), water, and sodium hydroxide, with different ratios and different orders of addition, resulted in different formulas. Cooper et al. reported the O-coordinated Cr(III) dinicotinato complex with the formula $[Cr(nic)_2(OH_2)_3(OH)]$ (nic = nicotinato(−)).[11] This complex was prepared by addition of sodium nicotinate to a hot solution of Cr(III) nitrate in a 1:2 Cr to nicotinate molar ratio, which when cooled gave a blue precipitate.[11] Another preparative method, reported by Evans and Pouchnik, involved heating an aqueous solution of Cr(III) chloride and nicotinic acid to 333 K; then the pH value was adjusted to 7.5 by NaOH to give a precipitate.[16] The formula of the product depended on the molar ratio of Cr to nicotinic acid, i.e., $[Cr(nic)(H_2O)_3(OH)_2] \cdot H_2O$ for a 1:1 ratio and $[Cr(nic)_2(H_2O)_3(OH)] \cdot H_2O$ for 1:2 and 1:3 ratios.[16] However, a different formula of the product from the 1:2 Cr to nicotinic acid ratio, $[Cr(nic)(H_2O)_3(OH)_2]$,

Received: July 29, 2014
Published: September 15, 2014

was reported by Rhodes et al.[17] The patented procedure that is used to prepare the commercial Cr(III) nicotinato complex (Chromemate, InterHealth) involves addition of the Cr(III) salt solution (CrX_3) to a solution of alkali metal salt of nicotinic acid.[10] This method leads to formation of an intense purple solid in a purple solution.[10] The purple solid was purported to be a mixture of Cr(III) trinicotinato and Cr(III) dinicotinato monochloride.[10] Using the same preparative method, Rhodes et al. reported that the purple products were polymers with the formula $[Cr(nic)_2(OH_2)_x(OH)]_n$ that precipitated along with some [nicH]X, which can be removed by subsequent solvent extraction.[17] Due to the fact that all of the Cr(III) nicotinato complexes are extremely insoluble in water and other common solvents and decompose in dimethyl sulfoxide (DMSO), their characterization has been limited. The results from infrared spectra of these solids revealed that the nicotinates coordinate with Cr through the carboxylato oxygen atoms.[11,17] Other characterization techniques, such as UV−vis, MS, and NMR spectroscopies, were applied using the solutions before neutralization or by dissolving the solids in hydrochloric acid,[17] which changed the structures of the compounds.

Despite the widespread commercialization of these supplements for many years, they resisted structural characterization. Here we describe the use of X-ray absorption spectroscopy (XAS), including X-ray absorption near-edge structure (XANES) and extended X-ray absorption fine structure (EXAFS), which is a widely used technique for characterizing metal centers in coordination compounds.[18−20] Multiple scattering (MS) analysis of EXAFS data, in combination with XANES and other spectroscopic techniques, such as UV−vis, IR, and EPR spectroscopies, is a very powerful tool for determining the three-dimensional structures of metal complexes, especially when X-ray crystallographic structures are not available, and has been widely and successfully applied to Cr coordination chemistry.[19−21]

EXPERIMENTAL SECTION

Materials. The following reagents were used: $CrCl_3·6H_2O$ (*trans*-$[CrCl_2(OH_2)_4]Cl·2H_2O$, Riedel-de Haen, ≥96%), nicotinic acid (Fluka, ≥99), and NaOH (Merck, 99.99%). Water was purified using the Milli-Q technique.

Analytical Techniques. *Microanalysis.* Determination of C, H, and N was performed by the Microanalytical Unit, Research School of Chemistry, Australian National University (Canberra), using a Carlo Erba 1106 Automatic Analyzer. Determination of Cr was carried out using atomic absorption spectroscopy (a Varian AA800 spectrometer with acetylene/air flame atomization) after digestion of the samples with 69% HNO_3 (Merck).

UV−Vis Spectroscopy. Solid-state UV−vis spectra were obtained by the diffuse reflectance technique using the Kubelka-Monk function. Spectra were recorded at ∼293 K on a Varian Cary 5 UV−vis−NIR spectrophotometer over the range 250−800 nm.

Infrared Spectroscopy. Solid-state IR spectroscopy of the samples was performed on a FTS-40 BioRAD spectrometer. Spectra were recorded at ∼293 K in diffuse reflectance mode over the range 2000−400 cm^{-1} at 4 cm^{-1} resolution using KBr as a background.

EPR Spectroscopy. A Bruker EMX spectrometer equipped with a Bruker EMX 035 M NMR gaussmeter and a Bruker EMX 048T microwave frequency counter was used to record X-band EPR spectra of the solid Cr(III) complexes at ∼293 K. Chromium(III) nicotinato complexes were diluted with boron nitride (BN) in a 1:10 mass ratio. Experimental parameters were as follows: center field, 3500G; sweep width, 1000 G; resolution, 1024 points; microwave power, 2.0 mW; modulation frequency, 100 kHz; modulation amplitude, 5 G; receiver gain, 1×10^3 to 1×10^4; and microwave frequency, ∼9.74 GHz. EPR spectra were processed using WIN-EPR software.[22]

X-ray Absorption Spectroscopy. Chromium K-edge spectra were recorded at the Australian National Beamline Facility (ANBF), beamline 20B at the Photon Factory, Tsukuba, Japan, with a Si(111) monochromator. The beam energy was 2.5 GeV, and the maximum beam current was 400 mA. Samples were diluted with boron nitride (BN) in the ratio of 1:5. All XAS data were acquired in fluorescence detection mode using a 36-pixel Ge planar detector (Eurisys). XANES and EXAFS spectra were recorded over the energy ranges: 5770−6200 and 6050−7000 eV, respectively. The energy scale was calibrated using a stainless steel foil as an internal standard (calibration energy, 5989.0 eV, corresponding to the first peak of the first derivative of Cr(0) edge).[23] Calibration, averaging, splining, and calculations of theoretical EXAFS data were performed using the Xfit software package.[24] All parameters in the EXAFS equation were calculated ab initio using the multiple-scattering program FEFF6.01,[24,25] by which an experimental EXAFS spectrum could be fitted to the calculated spectrum of a structural model.[24] Fourier filtering was applied in calculations to reduce the noise in the EXAFS data at high k values.[24] Constraints and restraints were used to reduce the degrees of freedom of the model. In all models, similar bond lengths and angles were restrained to be equal (within 0.01 Å and 5°, respectively).[24] Debye−Waller factors were restrained to be within 0.001 and 0.02 $Å^2$, and those of similar atoms of the ligands were constrained to be equal. Cr−O bond lengths for the carboxylato, hydroxido, alkoxido, or aqua ligands and the Cr−N bond lengths for pyridine ligands were loosely restrained to be close to those found in the literature (within 0.05 or 0.1 Å).[26−28] The angles around the Cr center were restrained to be octahedral (within 10°). Initial models for Cr(III) nicotinato complexes were built using Chem3D Pro software.[29] Bond lengths and angles within nicotinato ligands were restrained to be close to those found in the crystal structures of nicotinic acid (within 0.05 Å and 5°, respectively).[30] The quality of the fits was determined by R values, in which smaller R values corresponded to a better fit, and the fits with $R < 20\%$ were considered good.[20] Errors in the estimated EXAFS parameters, arising from the noise in the data, were determined by Monte Carlo analysis within the Xfit software[24] and did not exceed the limits of expected systematic errors of MS XAFS calculations (±0.01−0.02 Å for bond lengths and ±2° for bond angles).[31] Fitting conditions were set as follows: k, 1−15 $Å^{-1}$; FT range, 1.0−5.0 Å; plane-wave path filter threshold, 2%; maximal effective path length of a photoelectron, 5.0 Å; curved-wave path filter threshold, 3%; maximum number of legs, 5; scale factor S_0^2, 0.9 ± 0.1. The models were overdetermined ($N_i/p > 1$, where N_i is the number of independent observations and p is the number of varied parameters) in the EXAFS calculations in order to obtain meaningful solutions.[20,32]

Principal Component Analysis (PCA). The PCA technique was applied to provide an objective visual representation of the relationships between samples and variables (e.g., IR, EPR spectral data) using the Unscrambler X software (CAMO software AS., Norway).[33] PCA takes information carried by the original variables and projects them onto a smaller number of latent variables called Principal Components (PC), in which the first PC (PC1) contains the greatest source of information in the data set and each subsequent PC (PC2, PC3, ...) contains, in order, less information than the previous one.[33]

Synthesis and Characterization. A series of Cr(III) nicotinato complexes was synthesized using literature procedures[11,16,17] by mixing a hot solution of $CrCl_3·6H_2O$ with a solution of nicotinic acid in molar ratios of 1:1, 1:2, or 1:3 Cr to nicotinic acid, respectively, and then adding a solution of NaOH dropwise to adjust the pH value to 4.0 or 7.0. Solids formed from different combinations of Cr and nicotinic acid, and different pH values were coded as **A1_4**, **A2_4**, **A3_4**, **A1_7**, **A2_7**, and **A3_7**, in which the first number indicates the molar ratio of nicotinic acid over Cr and the second number indicates the pH value of the solution from which the product was collected.

Specifically, nicotinic acid (5.0 mmol for **A1**, 10 mmol for **A2**, or 15 mmol for **A3**) was mixed with deionized water (10 mL), and the mixture was heated at 353 K with stirring. Separately, $CrCl_3·6H_2O$ (5.0 mmol) was added to deionized water (10 mL), and the mixture was

dx.doi.org/10.1021/ic501818w | *Inorg. Chem.* 2014, 53, 10685−10694

Table 1. Compositions of Cr(III) Nicotinato Complexes Synthesized by Different Methods

no.[a]	synthesis method[c]	ref[d]	calculated formula[e]	structure[f]
A1_4	nicH:Cr 1:1, pH 4	16,17	$[Cr(nic)(OH)_2(H_2O)]\cdot 0.1nicNa$[g]	
A1_7	nicH:Cr 1:1, pH 7	16,17	$[Cr_4(nic)_3(OH)_9(H_2O)_3]\cdot 1.5H_2O$	$1.5:1[Cr_2(\mu\text{-}OH)_2(\mu\text{-nic-}\kappa O{:}\kappa N)_2(OH)_2(H_2O)_2]_n{:}Cr(OH)_3$
A2_4	nicH:Cr 2:1, pH 4	16,17	$[Cr_2(nic)_3(OH)_3(H_2O)_2]\cdot 0.5H_2O\cdot 0.15nicNa$	
A2_7	nicH:Cr 2:1, pH 7	16,17	$[Cr(nic)(OH)_2(H_2O)]$	$[Cr_2(\mu\text{-}OH)_2(\mu\text{-nic-}\kappa O{:}\kappa N)_2(OH)_2(H_2O)_2]_n$
A3_4	nicH:Cr 3:1, pH 4	16,17	$[Cr(nic)_2(OH)(H_2O)]\cdot 0.5H_2O$	
A3_7	nicH:Cr 3:1, pH 7	16,17	$[Cr_2(nic)_3(OH)_2(H_2O)_2]$	$[Cr_2(\mu\text{-}OH)_2(\mu\text{-nic-}\kappa O{:}\kappa N)_3(H_2O)_2]_n$
A3b[b]	nicNa:Cr 3:1, patented product	10	$[Cr(nic)_2(OH)(H_2O)]\cdot 0.5H_2O$	$[Cr_2(\mu\text{-}OH)_2(nic\text{-}\kappa O)_2(\mu\text{-nic-}\kappa O{:}\kappa N)_2(H_2O)_2]_n$

[a]In the designations, the first number indicates the molar ratio between nicotinic acid and $CrCl_3\cdot 6H_2O$ used for synthesis and the second number indicates the pH at which product was isolated. [b]Cr(III) nicotinato was synthesized according to the patented method.[10] [c]The molar ratios of nicotinic acid and $CrCl_3\cdot 6H_2O$ and the pH conditions were used to obtain the products. [d]Literature references to the synthesis methods. [e]Formulas were calculated from the AAS and microanalysis results (Table S1, Supporting Information). [f]Structures assigned on the basis of the spectroscopic and EXAFS analyses reported herein. [g]The fitting for **A1_4** for the Cr content was off by ~1% (Table S1, Supporting Information).

heated at 353 K with stirring until the solid had completely dissolved. The latter solution was added with rapid stirring to the nicotinic acid solution, until a homogeneous solution was formed. Next, a NaOH solution (1.0 M) was added slowly to the reaction mixture to adjust the pH value to 4.0 or 7.0, and the resultant mixture was continued to be heated and stirred for a further 2 h. A gray-purple precipitate formed from a purple solution at pH 4.0, while at pH 7.0, the filtrate was colorless. The precipitate was filtered and washed three times with deionized water and then dried in the oven at 333 K overnight.

Chromium(III) nicotinato complex **A3b** was synthesized following the patented method.[10] Nicotinic acid (15 mmol) was added to 10 mL of deionized water containing NaOH (15 mmol). The mixture was heated at 353 K until the nicotinic acid had dissolved. On addition of a hot solution of $CrCl_3\cdot 6H_2O$ (5.0 mmol), a distinct purple precipitate was formed from the purple solution. The reaction mixture was continued to be heated for 2 h, and then the precipitate was filtered. The purple solid obtained was washed three times with deionized water and dried in the oven at 333 K.

The insolubility of these complexes in water, ethanol, methanol, and other common organic solvents prevented their characterization by common techniques such as solution UV–vis, ESMS, and NMR spectroscopies. Solid-state UV–vis, infrared spectra (IR), electron paramagnetic resonance (EPR), and X-ray absorption spectroscopies (XAS, including XANES and EXAFS) of Cr(III) nicotinato complexes were used to characterize the structures of these complexes (see Results).

RESULTS

Elemental Analysis. Elemental analysis results of these Cr(III) nicotinato complexes are shown in Table S1 (Supporting Information), and their calculated formulas are summarized in Table 1.

UV–Vis Spectroscopy. Solid-state UV–vis spectra of Cr(III) nicotinato complexes (Figure 1 and Table 2) were

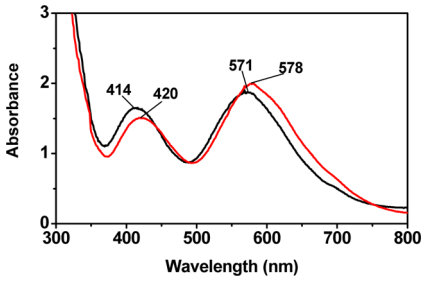

Figure 1. Solid-state UV–vis spectra of **A3b** (black line) and **A3_7** (red line). Spectra of other Cr(III) nicotinato complexes are given in Figure S1 (Supporting Information). Designations of the complexes correspond to those given in Table 1

Table 2. Peak Positions and Ligand-Field Parameters Obtained from Solid-State UV–Vis Spectra of Cr(III) Nicotinato Complexes

sample[a]	λ_1, nm ($^4T_{2g} \leftarrow {}^4A_{2g}$)	λ_2, nm ($^4T_{1g} \leftarrow {}^4A_{2g}$)	ν_1,10^3 cm^{-1} (Δ_o)	ν_2, 10^3 cm^{-1}	B, cm^{-1}
A1_4	579	421	17.27	23.75	636
A2_4	579	421	17.27	23.75	636
A3_4	576	419	17.36	23.87	638
A3b	571	414	17.51	24.16	653
A1_7	583	424	17.15	23.59	631
A2_7	579	421	17.27	23.75	636
A3_7	578	420	17.30	23.81	639

[a]Designations of the complexes correspond to those given in Table 1.

similar, with two absorbance maxima at about 420 (~23.8 × 10^3 cm^{-1}, ν_2) and 580 nm (~17.2 × 10^3 cm^{-1}, ν_1), assigned to $^4T_{1g} \leftarrow {}^4A_{2g}$ and $^4T_{2g} \leftarrow {}^4A_{2g}$ spin-allowed transitions, respectively. These two peaks in the spectrum of **A3b** shifted to lower wavelengths, 414 (~24.1 × 10^3 cm^{-1}; ν_2) and 571 nm (~17 × 10^3 cm^{-1}; ν_1), respectively. Spectra of **A3_7** and **A3b** are shown in Figure 1, and those of other Cr(III) nicotinato complexes are shown in Figure S1, Supporting Information. Peaks due to the formally spin-forbidden transitions were not resolved. The ligand field energies, $\Delta_o = 10Dq$ (corresponding to ν_1) and values of the Racah parameter, $B = (2\nu_1^2 + \nu_2^2 - 3\nu_1\nu_2)(15\nu_2 - 27\nu_1)$,[34,35] of the complexes are listed in Table 2. These show a trend whereby higher nicotinato ligand to Cr ratios caused the most pronounced blue shifts of the absorbance maxima. This is consistent with the structures (Table 1) determined by the various techniques described herein, since the Δ_o values for the spectrochemical series for Cr(III) follows the order $OH^- < RCO_2^- < OH_2 <$ pyridine. The highest ligand field is observed for **A3b**, which has a $[Cr(OH)_2(RCO_2)_2(OH_2)(Py)]$ chromophore and the weakest for **A1_7**, which has an average chromophore of $[Cr(OH)_{3.75}(RCO_2)_{0.75}(OH_2)_{0.75}(Py)_{0.75}]$.

IR Spectroscopy. Infrared spectra of nicotinic acid and **A3b** are shown in Figure 2, and spectra of other Cr(III) nicotinato complexes (Table 1) are given in Figure S2 (Supporting Information). Spectra of these complexes were very similar. Two strong absorption bands due to the asymmetric C=O and symmetric C–O stretching vibrations were observed near 1620 and 1375 cm^{-1}, respectively, while in the spectrum of nicotinic acid, the C=O stretching vibration occurs at 1717 cm^{-1}. Bands in the region of 2900–3500 cm^{-1} are associated with the O–H stretch of aqua and hydroxido ligands.[36]

dx.doi.org/10.1021/ic501818w | Inorg. Chem. 2014, 53, 10685–10694

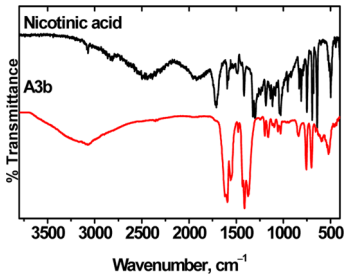

Figure 2. FTIR spectra of nicotinic acid (upper) and **A3b** (lower), which represents those of Cr(III) nicotinato complexes. Spectra of other Cr(III) nicotinato complexes are given in Figure S2 (Supporting Information). Designation of the complex corresponds to that given in Table 1.

PCA Analysis. PCA analysis was used in order to provide an objective assessment of structural differences and similarities among these Cr(III) nicotinato complexes. IR spectra of these complexes were normalized before performing the analysis, and the PC1 scores were plotted against PC2 in Figure 3. The PC1 described 74% of the variance in which Cr(III) nicotinato complexes obtained at pH 4.0 (**A1_4**, **A2_4**, **A3_4**, and **A3b**) were separated from those obtained at pH 7.0 (**A1_7**, **A2_7**, and **A3_7**). The separation of these samples along the PC1 axis was mainly due to the spectral data at 1375, 1410, and 1620 cm^{-1} (PC1 loadings, Figure 3). These frequencies represented the vibrations of COO^- groups and/or pyridine rings. The broad O−H stretches of aqua and hydroxido ligands at around 3000−3500 cm^{-1} also contributed to the separation of these compounds on PC1. Vibrations around 1375−1620 cm^{-1} and the broad O−H stretches led to the separation of **A1_4** from other compounds on PC2 (PC2 loadings plots, Figure 3).[36]

EPR Spectroscopy. EPR signals of Cr(III) nicotinato complexes (Table 1) were similar to each other and very broad with g values ≈ 1.97−1.99, which correspond to the signal of Cr(III) in octahedral geometry.[37] Typical EPR spectra of Cr(III) nicotinato complexes (**A3b** and **A3_7**) are shown in Figure 4a and 4b, and spectra of other Cr(III) nicotinato complexes are given in Figure S3, Supporting Information. EPR spectra of a dinuclear Cr(III) picolinato complex ($[Cr(pic)_2(OH)]_2$, Figure 4c)[27] and a trinuclear Cr(III) propionato complex ($[Cr_3O(EtCOO)_6(H_2O)_3](NO_3)$, EtCOO = propionate(−), Figure 4d)[38] were also recorded to compare with those of Cr(III) nicotinato complexes. The broad spectra of Cr(III) nicotinato complexes were similar to that of a dinuclear Cr(III) complex that has two hydroxido bridges, while these spectra were significantly different from that of the trinuclear Cr(III) complex.

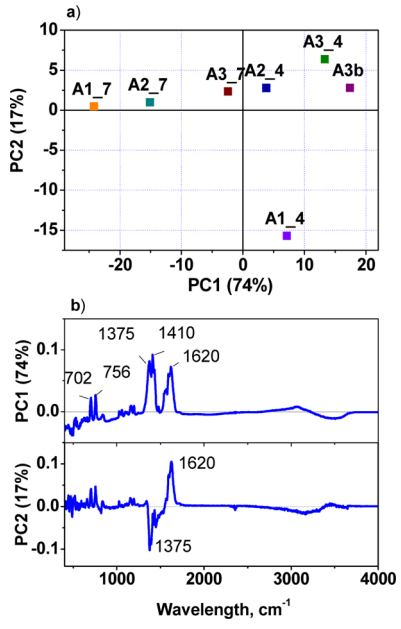

Figure 3. PCA scores plots from FTIR spectral data of Cr(III) nicotinato complexes using the Unscrambler X software: (a) PC1 vs PC2 scores; (b) PC1 and PC2 loadings. Designations of the complexes correspond to those given in Table 1

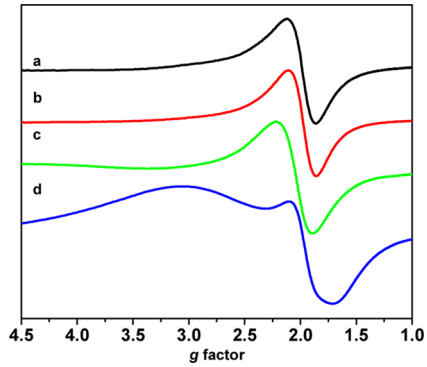

Figure 4. Typical EPR spectra of Cr(III) nicotinato complexes and dinuclear and trinuclear Cr(III) complexes obtained at room temperature: (a) **A3b**, (b) **A3_7**, (c) $[Cr(pic)_2(OH)]_2$, and (d) $[Cr_3O(EtCOO)_6(H_2O)_3]^+$. Spectra of other Cr(III) nicotinato complexes are given in Figure S3, Supporting Information. Designations of the complexes correspond to those given in Table 1.

When all EPR spectra of Cr(III) nicotinato complexes were normalized and plotted against g factors, subtle differences became evident (Figure S4, Supporting Information). As was the case for IR spectral analysis, PCA was also applied to obtain an objective analysis of the EPR spectra of Cr(III) nicotinato complexes to determine which species were closest in chemical structure. The scores of each sample on PC1 and PC2, which show the sample differences or similarities, were plotted in Figure 5. The PC1 explained 95% of the variance, in which the spectral data at g ≈ 2.0 contributed most to the separation of samples along the PC1 axis (Figure 5b).

The plot shows that at the same ratio of Cr and nicotinic acid increasing the pH values from 4.0 to 7.0 shifted the PC1 scores from left to right, corresponding to g factors shifted from higher to lower values. For complexes prepared under the same pH condition, increasing the ratio of nicotinic acid over Cr caused a shift of the PC1 scores to the left, which corresponded to a shift to higher g values (Figure 5a). The PC2 (2%) separated **A3b** from the other samples (Figure 5b) mainly due to the spectral data at g ≈ 1.96 (Figure 5c).

XANES Spectroscopy. XANES spectra at ∼293 K of Cr(III) nicotinato complexes obtained at pH 7.0 (**A1_7**, **A2_7**, and **A3_7**) and the spectrum of the patented Cr(III) nicotinato complex (**A3b**) are shown in Figure 6. XANES spectra of **A1_7**, **A2_7**, and **A3_7** were similar, with two main maximum peaks (features a and b, Figure 6). These spectra were different from that obtained from **A3b**, in which the maximum b of the XANES of **A3b** was more intense (feature b, Figure 6). Despite using the same nicotinic acid to Cr ratio, the XANES spectra of

dx.doi.org/10.1021/ic501818w | Inorg. Chem. 2014, 53, 10685−10694

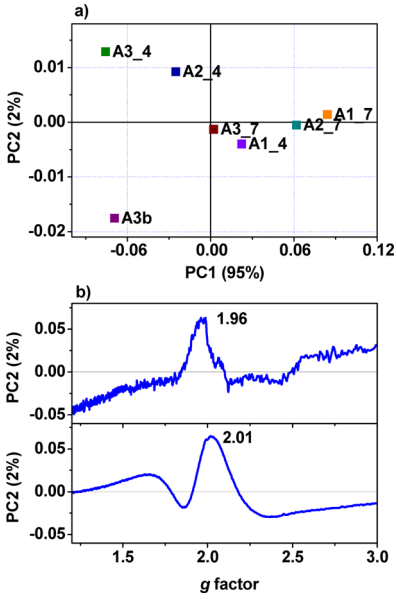

Figure 5. Plots of PCA scores plots and loadings from EPR data of Cr(III) nicotinato complexes using the Unscrambler X software: (a) PC1 vs PC2; (b) PC1 and PC2 loadings. Normalized EPR spectra used for this analysis are given in Figure S4 (Supporting Information). Designations of the complexes correspond to those given in Table 1

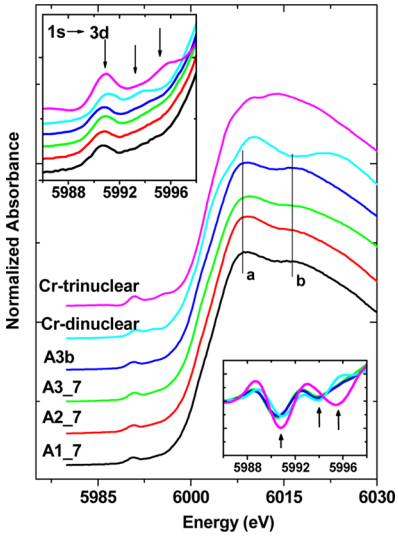

Figure 6. Comparison of Cr K-edge XANES spectra at ~293 K of Cr(III) nicotinato complexes prepared by different methods and those of dinuclear ($[Cr(pic)_2(OH)]_2$) and trinuclear ($[Cr_3O(EtCOO)_6(H_2O)_3]^+$) Cr(III) complexes. Designation of the complexes corresponds to those given in Table 1. All samples were diluted with BN in 1:50 mass ratio in order to record the XAS spectra. (Inset) (top) Expanded view of the pre-edge region and (bottom) second derivative of the pre-edge data.

A3_7 and **A3b** were significantly different. Interestingly, the intensity of the spectra at the edge decreased with an increase in the nicotinic acid:Cr ratio. The edge energies of these complexes (obtained from the first derivative spectra) were at ~6002 eV (Table 3). The pre-edge regions of these complexes, which represent symmetry-forbidden 1s → 3d transitions, showed a weak pre-edge peak at ~5991 eV (Table 3) and a less prominent peak at ~5994 eV (Figure 6, top inset). The later peak was only clearly shown in the second derivative of the

Table 3. XANES Edge and Pre-Edge Energy of Cr(III) Nicotinato Complexes

sample	E_0[a] (eV)	$E_{pre\text{-}edge}$[b] (eV)	$\Delta E_{pre\text{-}edge}$[c] (eV)
A1_7	6002.0	5990.7, 5993.9	3.2
A2_7	6001.9	5990.8, 5994.0	3.2
A3_7	6001.7	5990.8, 5994.0	3.2
A3b	6001.8	5990.8, 5994.0	3.2
$[Cr(pic)_2(OH)]_2$	6002.0	5991.0, 6993.8	2.8
$[Cr_3O(EtCOO)_6(H_2O)_3]^+$	6002.2	5990.8, 5995.6	4.8

[a]Edge energies were obtained from the first derivative of the XANES spectra. [b]Pre-edge energies from the second derivatives of the pre-edge spectra. [c]Peak energy differences from the second derivatives of the pre-edge spectra.

XANES data (Figure 6, bottom inset). The pre-edge features of the spectrum of the dinuclear Cr(III) complex ($[Cr(pic)_2(OH)]_2$) were similar to those of Cr(III) nicotinato complexes, but those of trinuclear Cr(III) complex ($[Cr_3O(EtCOO)_6(H_2O)_3]^+$) were different (Figure 6). The pre-edge peaks of $[Cr_3O(EtCOO)_6(H_2O)_3]^+$ were more intense, with greater energy difference of the pre-edge peaks (~5 eV, compared to ~3 eV in the spectra of Cr(III) nicotinato complexes, Table 3).

EXAFS Structural Analyses. All EXAFS spectra were analyzed using the same k range (0−15 Å^{-1}) to provide a valid comparison of the Fourier transform (FT) of the EXAFS (Figure 7). There was one main peak at 1.55 Å (phase shift not corrected) in the FTs of all types of Cr(III) nicotinato complexes, corresponding to the first coordination shell of Cr···O/N interactions. The FTs clearly show that the intensity of this peak was higher in **A1_7** and **A2_7** compared to **A3_7** and **A3b**. Another important feature observed in the FTs is the weak peak at ~2.71 Å for all of the Cr(III) nicotinato complexes. These peaks could be Cr···Cr interactions and/or multiple scattering (MS) contributions.[21] On the basis of elemental analysis results (Tables 1 and S1, Supporting

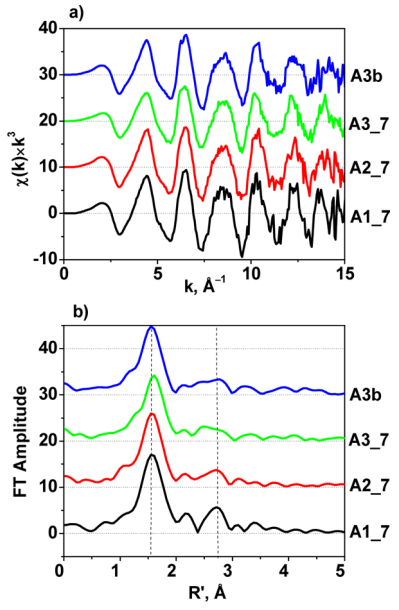

Figure 7. Comparison of (a) k^3-weighted EXAFS and (b) Fourier transform (FT) of k^3-weighted EXAFS spectra of Cr(III) nicotinato complexes at ~293 K. Designations of the complexes correspond to those given in Table 1.

dx.doi.org/10.1021/ic501818w | Inorg. Chem. 2014, 53, 10685−10694

Information), several models of Cr(III) nicotinato complexes were used for MS analysis of their EXAFS spectra, including mononuclear, dinuclear, and trinuclear cores. A fit was considered good if it had $R < 20\%$, the scale factor $S_0^2 = 0.9 \pm 0.1$, and acceptable Debye–Waller factors, σ_i^2.[20] Only models of the dihydroxido-bridged dinuclear Cr core in which each of the remaining octahedral sites around the Cr atom was surrounded by pyridine *N* donors and carboxylato and aqua *O* donors (models **I**–**III** in Figure 8, and models in Figure S5, Supporting Information) gave reasonable fits for the EXAFS of Cr(III) nicotinato complexes (**A3b**, **A3_7**, **A2_7**, and **A1_7**).

Model **I** (Figure 8) and its isomers (**Ia**–**Ic**, Figure S5, Supporting Information) are consistent with the stoichiometry for $[Cr(nic)_2(OH)(H_2O)_2]_n$, in which one O-bound nicotinato ligand from each Cr is nonbridging and the remaining nic ligands form bridges to other dihydroxido dimers. Model **II** (Figure 8) and its isomers (**IIa**–**IIf**, Figure S5, Supporting Information) fit the stoichiometry for $[Cr_2(nic)_3(OH)_2(H_2O)_2]_n$, while model **III** (Figure 8) and its isomers (**IIIa**–**IIIb**, Figure S5, Supporting Information) fit the stoichiometry for $[Cr(nic)(OH)_2(H_2O)]_n$.

All nicotinato ligands in models **II** and **III** and their isomers act as bridging ligands between dinuclear cores. When aqua ligands in models **I** and **II** were replaced by nicotinato ligands (model **IV**, Figure S5, Supporting Information), worse fits resulted, even though more fitting parameters were involved. This and the stoichiometry of the formulas are consistent with the binding of aqua ligands in these complexes.

The conditions, constraints, and restraints used in the MS calculation of the EXAFS spectra of Cr(III) nicotinato complexes are given in Tables S2–S4 (Supporting Information). In model **II**, two Cr sites of the dinuclear core are not symmetrical; therefore, EXAFS analysis was fitted using two absorbing atom sites (Cr^0 and Cr^{22}, model **II** in Figure 8), while one absorber site was applied in the fits to models **I** and **III** (Figure 8) and **IV** (Figure S5, Supporting Information). A comparison of fitting parameters between these models is given in Table S5 (Supporting Information). For **A3b** the best fit to the EXAFS data was obtained with model **I** ($R = 12.5\%$), Model **II** gave the best fit to **A3_7** ($R = 18.7\%$), while **III** gave the best fits to **A2_7** and **A1_7** ($R = 17.5\%$ and 19.3%, respectively). Experimental and calculated EXAFS and FT of EXAFS spectra of these complexes obtained from the best fits are shown in Figure 9. The most significant photoelectron scattering paths contributing to the calculated EXAFS spectra of the Cr(III) nicotinato complexes are described in Tables

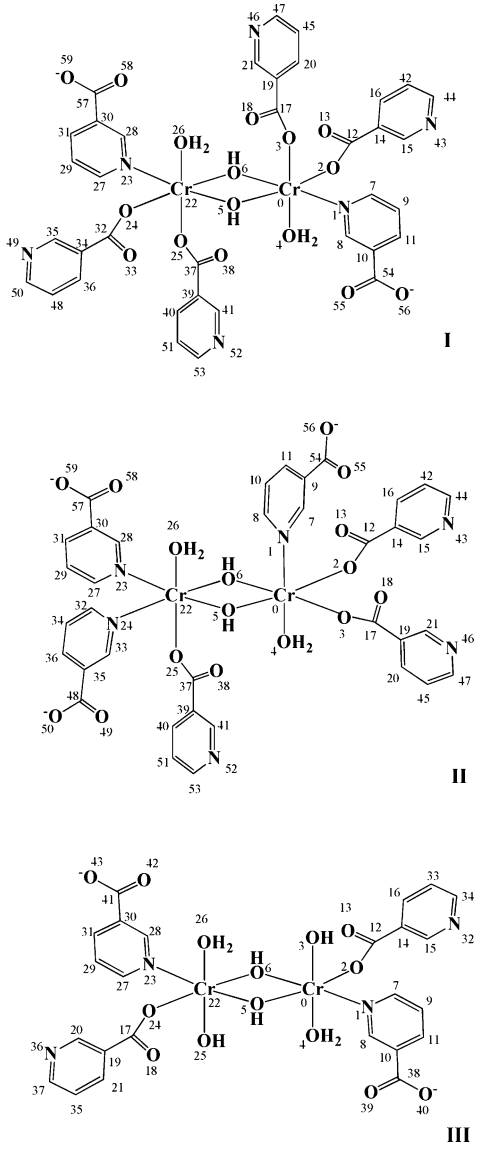

Figure 8. Models of the dinuclear Cr(III) nicotinato cores for the nicotinato-bridged polymers which gave the best fits in MS EXAFS calculations of **A3b**, **A3_7**, **A2_7**, and **A1_7**. Atom numbering corresponds to that used in Tables S2–4 (Supporting Information). Models that provided the best fits to the EXAFS for **A3b**, **A3_7**, **A2_7**, and **A1_7** were models **I**, **II**, **III**, and **III**, respectively.

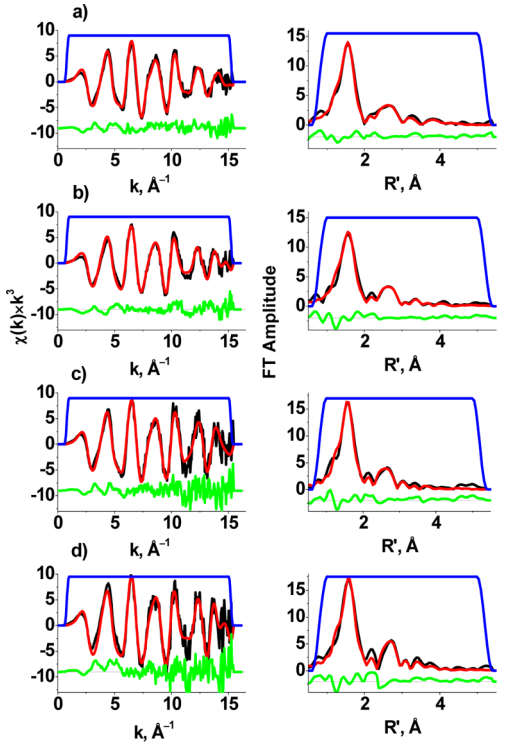

Figure 9. Observed (black), calculated (red), and residual (green) spectra and the window function (blue) for EXAFS (left) and FT EXAFS (right) spectra of (a) **A3b** ($R = 12.5\%$), (b) **A3_7** ($R = 17.2\%$), (c) **A2_7** ($R = 17.5\%$), and (d) **A1_7** ($R = 19.3\%$). Calculation details are given in Table S3 (Supporting Information). Designations of the complexes correspond to those given in Table 1.

dx.doi.org/10.1021/ic501818w | *Inorg. Chem.* 2014, 53, 10685–10694

Table 4. Fit Parameters, Bond Angles, and Bond Lengths Obtained from MS EXAFS Analysis of Cr(III) Nicotinato Complexes[a]

	A3b	A3_7	A2_7	A1_7
parameters				
$-\Delta E_0$ (eV)	1.82(1)	0.74(1)	2.0(1)	1.6(1)
S_0^2	0.87(5)	0.93(9)	0.87(1)	0.95(5)
R (%)	12.5	18.7	17.5	19.3
σ_i^2 (Å^2)	0.0009−0.0200[b]	0.0010−0.0087	0.0009−0.0200[b]	0.0009−0.0200[b]
model	I	II	III	III
bond lengths (Å)				
Cr^0−N^1	2.06(1)	2.03(1)	2.04(1)	2.04(1)
Cr^0−O^2	1.97(1)	1.98(2)	1.97(1)	2.00(1)
Cr^0−O^3	2.01(2)	1.95(1)	1.97(1)	1.97(1)
Cr^0−O^4	1.93(1)	1.98(1)	1.98(1)	2.00(2)
Cr^0−O^5	1.96(1)	1.92(1)	1.95(1)	1.92(1)
Cr^0−O^6	1.93(1)	1.95(1)	1.94(1)	1.92(1)
Cr^0−Cr^{22}	2.93(2)	2.96(1)	2.95(1)	2.97(1)
bond angles (deg)				
N^1−Cr^0−O^2	91.3(3)	90.9(3)	91.5(1)	92.9(3)
N^1−Cr^0−O^3	91.6(5)	90.6(4)	90.9(4)	92.5(5)
N^1−Cr^0−O^4	178.6(4)	179.5(4)	89.7(4)	91.9(5)
N^1−Cr^0−O^5	91.3(3)	89.6(3)	93.2(3)	94.3(4)
N^1−Cr^0−O^6	90.8(3)	90.0(3)	175.7(3)	172.8(4)
O^2−Cr^0−O^3	92.0(5)	91.0(4)	90.6(4)	91.0(5)
O^2−Cr^0−O^4	89.4(4)	88.9(4)	89.1(4)	90.2(6)
O^2−Cr^0−O^5	174.2(3)	174.0(3)	175.1(3)	172.8(4)
O^2−Cr^0−O^6	92.4(3)	93.2(3)	92.6(3)	94.3(5)
O^3−Cr^0−O^4	89.6(6)	88.9(5)	179.3(6)	175.3(7)
O^3−Cr^0−O^5	93.1(5)	94.9(4)	90.8(5)	88.9(6)
O^3−Cr^0−O^6	174.9(5)	175.6(4)	90.3(5)	87.5(6)
O^4−Cr^0−O^5	87.8(4)	90.6(4)	89.5(5)	89.4(6)
O^4−Cr^0−O^6	87.9(4)	90.4(4)	89.1(5)	87.9(6)
O^5−Cr^0−O^6	82.4(3)	80.9(3)	82.7(4)	78.5(5)
Cr^0−O^5−Cr^{22}	97.6(4)	99.9(5)	97.1(3)	101.4(5)
Cr^0−O^6−Cr^{22}	97.6(4)	99.0(5)	97.1(3)	101.4(5)

[a]Designations of the parameters: $\Delta E_0 = E_0 - 6005$ eV, where E_0 is the threshold energy; S_0^2 is a scale factor; R is the goodness of fit; and σ_i^2 are the Debye−Waller factors. Standard deviations in the least significant figure (given in parentheses), arising from the noise in the data, were estimated by the Monte Carlo method.[24] Expected systematic errors are 0.01−0.02 Å for bond lengths and 2° for bond angles.[31] Calculation details are given in Tables S2 and S4 (Supporting Information). Atom numbering corresponds to the models given in Figure 8. Designations of the complexes correspond to those given in Table 1. [b]These values were generally between around 0.001 and 0.007 Å^2, but one or two of the most distant atoms on the second Cr in each model that were over 4 Å away from the absorber had values of approaching or equal to 0.02 Å^2, but these had very little contributions to the overall scattering (Tables S10 and S11 (Supporting Information)).

S6−S9 (Supporting Information). Fitting parameters as well as calculated bond angles and bonds lengths around the Cr center obtained from the best fits of MS EXAFS analysis of **A3b**, **A3_7**, **A2_7**, and **A1_7** are given in Table 4.

Details of other bond lengths, bond angles, and Debye−Waller factors, including those in the ligands, are listed in Tables S10 and S11 (Supporting Information). Cr−N (pyridine) distances were the same within experimental error, 2.05 Å in **A3b**, 2.03 Å in **A3_7**, and 2.04 Å in **A2_7** and **A1_7**. The different Cr−O(carboxylato) bond lengths in **A3b** (1.97 and 2.01 Å) can be explained by the differences between two nicotinato ligands: one acted as a bridge, while the other was nonbridging. These bonds in **A3_7** were similar within experimental error (1.95 and 1.98 Å), as both nicotinato ligands bridged to other Cr atoms. The bond lengths between Cr and two hydroxido bridges were equal in **A2_7** and **A1_7**, ∼1.94 and 1.92 Å, respectively, while these values in **A3b** and **A3_7** were different. The Cr···Cr distance in the dinuclear core of **A3b** (∼2.93 Å) was slightly, but not significantly, shorter than those found in **A3**−**7**, **A2_7**, and **A1_7** (∼2.95 Å).

Cr−OH−Cr bridging angles were in the range of 98−101°. It was not possible to distinguish between aqua and nonbridging hydroxido ligands in MS analyses of **A2_7** and **A1_7** since they only differ by one H atom, which would not have a significant contribution to the EXAFS for these structures, and the distances from these ligands to Cr center were in the range of 1.97−2.00 Å.

DISCUSSION

Nicotinato Cr(III) compounds were initially purported to be components of the GTF[1] and ill-defined Cr(III) nicotinato complexes are still used as dietary supplements, even though the purported GTF has long been shown to be an artifact.[39] It was reported that different methods of preparation of the nicotinato complexes gave different compounds, which were polymers of Cr(III), oxygen-bound nicotinato, hydroxido, and aqua ligands with 1:1 or 1:2 Cr to nicotinato ratios.[17] However, until the results reported here, their structures have not been elucidated due to their insolubility and a lack of a suitable method for growing single crystals.

dx.doi.org/10.1021/ic501818w | Inorg. Chem. 2014, 53, 10685−10694

Previous spectroscopic studies on solutions from which Cr(III) nicotinato complexes precipitate, or on the species obtained by dissolving Cr(III) nicotinato in 1 M HCl,[17] did not provide detailed information on the structures of the polymers used in the supplements. In this study, from elemental analysis results, it was found that when increasing the pH value of the reaction from which the precipitate formed, the ratio of nicotinato ligands compared to Cr in the product decreased, probably due to protonation of the carboxylic acid group, whereas this ratio at the same pH value increased with an increase in the nicotinic acid to Cr reagent ratio, as expected.

The formulas of the products obtained from 1:1, 2:1, and 3:1 nicotinic acid to Cr molar ratios at pH 7 were $[Cr_4(nic)_3(OH)_9(H_2O)_3]\cdot 1.5H2O$, $[Cr(nic)(OH)_2(H_2O)]$, and $[Cr_2(nic)_3(OH)_2(H_2O)_2]$, respectively, which were not in agreement with the results reported by Evans and Pouchnik.[16] The reported formulas of $[Cr(nic)(H_2O)_3(OH)_2]\cdot H_2O$ for the 1:1 and $[Cr(nic)_2(H_2O)_3(OH)]\cdot H_2O$ for the 2:1 and 3:1 nicotinic acid to Cr ratios[16] were only obtained in our studies at pH ≈ 4 for the 1:1 and 3:1 molar syntheses, respectively. The found formula for the 2:1 synthesis at pH 7 was similar to that reported by Rhodes et al.[17] ($[Cr(nic)(OH)_2(H_2O)_3]$). The patented synthesis procedure[10] produced the same formula $[Cr(nic)_2(OH)(H_2O)]\cdot 0.5H_2O$ as that produced from the synthesis from nicotinic acid and Cr in 3:1 molar ratio at pH ≈ 4.

The results of MS analysis of the EXAFS spectra of **A1_7**, **A2_7**, **A3_7**, and **A3b** provided strong evidence that these compounds are polymers of dihydroxido-bridged dinuclear cores, in which nicotinato anions bridge adjacent Cr(III) atoms through both the pyridine N atom and the carboxylato O atom. In the structure of **A3b**, each Cr binds to three nicotinato ligands, among which only two act as bridges between dinuclear cores. Typical Cr···Cr distances found in different Cr complexes with different bridging groups are summarized in Table 5, which shows that Cr···Cr distances of dihydroxido-bridged Cr complexes are 2.93−3.01 Å.[27,38,40−51] Thus, all of the fitted Cr−L bond lengths and angles obtained from MS analysis are consistent with structures **I**−**III** or their geometric isomers and not other types of bridged polymers. The bond lengths and angles within the dinuclear core unit, including Cr−OH distances and Cr−OH−Cr and HO−Cr−OH angles, obtained from MS analysis (Table 4) are in agreement with those reported in crystallographic studies on hydroxido-bridged dinuclear Cr(III) complexes (1.92−1.99 Å for Cr−OH, 97.6−104.1° for Cr−OH−Cr, and 75.9−82.4° for HO−Cr−OH).[27,41,49−52] Similarly, the Cr−N distances are similar to those found in mononuclear and dinuclear Cr(III) picolinate complexes (2.05−2.07 Å),[27] and the Cr−O (carboxylato) bond lengths are within the ranges of Cr−O (carboxylato) distances for carboxylato Cr(III) complexes (1.93−2.01 Å).[27,39,48−52] When combined with elemental analyses (Table 1 and S1 (Supporting Information)) and EPR spectra, there are relatively few possibilities for appropriate models that are consistent with all the data. Of these, the best fits to the EXAFS were consistent with the following formulas for **A3b**, **A3_7**, and **A2_7**: $[Cr_2(\mu\text{-}OH)_2(nic\text{-}\kappa O)_2(\mu\text{-}nic\text{-}\kappa O{:}\kappa N)_2(H_2O)_2]_n$, $[Cr_2(\mu\text{-}OH)_2(\mu\text{-}nic\text{-}\kappa O{:}\kappa N)_3(H_2O)_2]_n$, and $[Cr_2(\mu\text{-}OH)_2(\mu\text{-}nic\text{-}\kappa O{:}\kappa N)_2(OH)_2(H_2O)_2]_n$, respectively; whereas **A1_7** is most likely to be a mixture of $[Cr_2(\mu\text{-}OH)_2(\mu\text{-}nic\text{-}\kappa O{:}\kappa N)_2(OH)_2(H_2O)_2]_n$ and $Cr(OH)_3$. The differences in the structure of **A3b** explained its separation from other compounds in PCA analyses of both EPR and IR spectra (Figures 3 and 5, except along PC1 for **A3_4**, which had a similar formula) as well as in its different UV−vis maxima (Figure 1). The higher g value in the EPR spectrum of **A3b**, compared to those of other Cr(III) nicotinato complexes, which means higher splitting energy,[53] is consistent with its lower λ_{max} values in the UV−vis spectra (Figures S1 and S4 (Supporting Information)).

PCA analysis of the EPR data of Cr(III) nicotinato complexes (Figure 5) showed the relationships between the EPR spectral data and either the pH or the nicotinic acid:Cr ratio. With regard to elemental analyses, when the ratio between nicotinato ligands and Cr decreases, the PC1 score is shifted to the right, which means there is a decrease in the g values, i.e., a decrease in Δ_o.[53] In the series, **A1_7**, **A2_7**, and **A3_7**, the value of Δ_o increased from **A1_7** to **A3_7**. These results are consistent with the maxima found in the UV−vis spectra of these complexes, in which the Δ_o value of **A3_7** was slightly higher than those of **A1_7** and **A2_7** (Table 3). These changes in band energies are due to the ligand field of the *O*-nicotinato ligand (RCO_2^-) being higher than that of OH^- ligand in the spectrochemical series, as polyatomic ligands usually cause stronger perturbations than monatomic ions.[54] Previous studies on the XANES spectra of Cr(III) complexes with a wide range of donor groups have shown a correlation between the edge energies and donor atoms.[21] The differences in the edge energies found in XANES spectra of these complexes (Figure 6) were too small (∼0.1−0.2 eV) to correlate the ligand field strength with the edge energy. However, when compared with the XANES spectra of O/N-donor and O-donor complexes reported previously,[23] it shows that these edge energies were in agreement with those of O/N-donor complexes: 6001.4 eV for $[Cr(phen)_2(dpp)_2]^+$ (phen = 1,10-phenanthroline, dpp = diphenylphosphato(1−)); 6001.6 eV for $[Cr(his)_2]^+$ (his = L-histidinato(1−)) and $[Cr(pic)_3]$ (pic = picolinato(1−)); 6001.8 eV for $[Cr(ala)_3]$; and 6002 eV for $[Cr(asp)_2]^-$ (asp = L-aspartato(2−)).[23] The higher intensity of the white lines observed in XANES spectra of **A1_7** and **A2_7** compared to those of **A3_7** and **A3b** is probably caused by OH^- ligands, as similar observations were reported in previous work where the white line intensity of the [Cr-

Table 5. Typical Cr···Cr Distances in Multinuclear Cr(III) Complexes with Different Bridging Groups

compound[a]	bridging groups	Cr···Cr (Å)	ref
$[Cr_2(OH)(CH_3CO_2)(nta)_2]^{2-}$	OH^-, $RCOO^-$	3.49	40
$[Cr_2(OH)_2(pic)_4]$	$2OH^-$	3.00	27
$[Cr_2(OH)_2(nta)_2]^{2-}$	$2OH^-$	2.96	41
$[Cr_2(OH)_2(nta)_2]^{2-}$	$2OH^-$	2.93	51
$[Cr_2O(NH_3)_{10}]^{4+}$	O^{2-}	3.64	42
$[Cr_2(OH)(NH_3)_9(H_2O)]^{5+}$	OH^-	3.87	42
$[Cr_2(OH)_2(nta)(tn)_2]^+$	$2OH^-$	2.98	43
$[Cr_2(OH)_2(nta)(phen)_2]^+$	$2OH^-$	2.96	44
$[Cr_2(OH)_2(OH_2)_8]^{4+}$	$2OH^-$	2.97	45
$[Cr_2(OH)(HCO_2)_2(OH_2)_6]^+$	$2OH^-$, $2RCOO^-$	3.38	46
$[Cr_3O(EtCO_2)_6(OH_2)_3]^+$	O^{2-}, $2RCOO^-$	3.27	37
$[Cr_3O(PhCO_2)_6(py)_3]^+$	O^{2-}, $2RCOO^-$	3.27	45
$[Cr_2(OH)_2(pda)_2(OH_2)_2]$	$2OH^-$	3.01	48
$[Cr_2(OH)_2(HCO_2)(bispma)_2]^{3+}$	$2OH^-$, $HCOO^-$	2.94	49

[a]Ligands: nta = nitrilotriacetato(3−); pic = picolinato(1−); tn = propane-1,3-diamine; phen =1,10-phenanthroline; EtCOO = propanoato(−); PhCOO = benzoato(−); py = pyridine; pda = pyridine-2,6-dicarboxylato(2−); bispma = bis[2-pyridylmethylamine].

dx.doi.org/10.1021/ic501818w | Inorg. Chem. 2014, 53, 10685−10694

$(OH)_6]^{3-}$ complex was much higher than that of Cr(III) amino acid complexes.[23] Thus, all of these data were consistent with the proposed structures.

In terms of gastrointestinal absorption, these insoluble Cr(III) nicotinato polymers are decomposed in the acidic environment of the stomach to allow absorption of discrete Cr complexes. The structures of these complexes formed under biologically relevant conditions are under investigation and will be published in the near future.

CONCLUSIONS

Cr(III) nicotinato complexes were synthesized by heating solutions of nicotinic acid and $CrCl_3 \cdot 6H_2O$ in 1:1, 2:1, and 3:1 molar ratios, followed by adjustment of the pH values to 4 or 7. These complexes are polymers of dihydroxido-bridged dinuclear Cr cores. Increasing the nicotinic acid to Cr ratios led to an increase in the number of nicotinato ligands bound to the Cr center, whereas increasing the pH value of the reaction mixture led to a reduced number of nicotinato ligands in the complexes. The local structures of Cr(III) nicotinato complexes obtained at pH 7 (**A3_7**, **A2_7**, and **A1_7**) and the patented complex (**A3b**) were characterized by performing MS analysis of their EXAFS spectra. Spectra of all four compounds were fitted well with dihydroxido-bridged dinuclear Cr models, in which each Cr was surrounded by two carboxylato O donors, one pyridine N donor, and one aqua ligand for **A3b** and **A3_7**, or by one carboxylato O donor, one pyridine N donor, one hydroxido, and one aqua ligand for **A2_7** and **A1_7**. Each dinuclear core is bridged to another through the nicotinato ligands. The main difference between **A3b** and the other three complexes is that each Cr has one nonbridging nicotinato ligand in **A3b**, whereas in the other complexes all of the nicotinato ligands are bridging. Results from UV−vis, FTIR, and EPR spectroscopies of these complexes were consistent with the nature of ligands found in EXAFS analysis. Determination of the structures of the Cr−nicotinato complexes will contribute to an understanding of the chemistry that ensues when these supplements interact with gastric acid in order to break down the polymers into water-soluble complexes that then can be absorbed. Our research in this area will be the subject of a future paper.

ASSOCIATED CONTENT

Supporting Information

Elemental analyses and UV−vis, IR, and EPR spectroscopy data; details of constraints and restraints used in MS analysis of EXAFS; comparison of fitting parameters using models in Figure 8. This material is available free of charge via the Internet at http://pubs.acs.org.

AUTHOR INFORMATION

Corresponding Author

*E-mail: peter.lay@sydney.edu.au.

Author Contributions

This project was formulated by P.A.L., A.L., and T.H.N.P. This manuscript is based on the Ph.D. research of T.H.N.P., who also prepared an initial draft of the manuscript with the assistance of the other authors. All other authors assisted T.H.N.P. in gathering the XAS data and provided expertise in certain aspects of data analysis. All authors contributed to the final versions of the manuscript, and all authors have given approval to the final version of the manuscript.

Notes

The authors declare no competing financial interest.

ACKNOWLEDGMENTS

This research was supported by Australian Research Council (ARC) Discovery Grants (DP0774173, DP0984722, and DP1095310), an ARC Professorial Fellowship (DP0984722) to P.A.L., and ARC LIEF grants for the EPR instrumentation. This research was undertaken, in part, at the Australian National Beamline Facility (ANBF) at the Photon Factory in Japan, operated by the Australian Synchrotron. We acknowledge the Linkage Infrastructure, Equipment and Facilities Program of the ARC for financial support (proposal numbers LE0989759 for access and LE0346515 for the 36-pixel Ge detector) and the High Energy Accelerator Research Organisation (KEK). We thank Drs. Garry Foran, James Hester, Celesta Fong, and Michael Cheah for assistance with XAS experiments at ANBF and Dr. Elizabeth Carter for assistance with the Varian Cary 5 UV−vis−NIR spectrophotometer.

REFERENCES

(1) Vincent, J. B. In *The Nutritional Biochemistry of Chromium(III)*; Vincent, J. B., Ed.; Elsevier: Amsterdam, 2007; pp vii−ix.
(2) Mertz, W.; Schwarz, K. *Arch. Biochem. Biophys.* **1955**, *58*, 504−506.
(3) Schwarz, K.; Mertz, W. *Arch. Biochem. Biophys.* **1957**, *72*, 515−518.
(4) Levina, A.; Codd, R.; Dillon, C. T.; Lay, P. A. *Prog. Inorg. Chem.* **2003**, *51*, 145−250.
(5) Vincent, J. B. *Dalton Trans.* **2010**, *39*, 3787−3794.
(6) (a) Levina, A.; Lay, P. A. *Chem. Res. Toxicol.* **2008**, *21*, 563−571. (b) Lay, P. A.; Levina, A. In *Binding, Transport and Storage of Metal Ions in Biological Cells*; Maret, W., Wedd, A. Eds.; RSC: Cambridge, U.K., 2014; Chapter 7, pp 188−222. (c) Lay, P. A.; Levina, A. In *Encyclopedia of Inorganic and Bio-inorganic Chemistry*,; Scott, R. A., Ed.; Wiley: Chichester, U.K., 2012; DOI: 10.1002/9781119951438.eibc0040.pub2.
(7) (a) Levina, A.; Lay, P. A. *Dalton Trans.* **2011**, *40*, 11675−11686. (b) Levina, A.; Mulyani, I.; Lay, P. A. In *The Nutritional Biochemistry of Chromium(III)*; Vincent, J. B., Ed.; Elsevier: Amsterdam, 2007; pp 225−256. (c) Mulyani, I.; Levina, A.; Lay, P. A. *Angew. Chem., Int. Ed.* **2004**, *43*, 4504−4507.
(8) Stearns, D. M. In *The Nutritional Biochemistry of Chromium(III)*; Vincent, J. B., Ed.; Elsevier: Amsterdam, 2007; pp 209−224.
(9) Vincent, J. B. *Polyhedron* **2001**, *20*, 1−26.
(10) Jensen, N. L. WO 8910357; Chromium nicotinate as synthetic glucose tolerance factor and its preparation. *Chem. Abstr.* **1989**, *113*, 171885.
(11) Cooper, J. A.; Anderson, B. F.; Buckley, P. A.; Blackwell, L. F. *Inorg. Chim. Acta* **1984**, *91*, 1−9.
(12) Bagchi, D.; Bagchi, M.; Balmoori, J.; Ye, X.; Stohs, S. J. *Res. Commun. Mol. Pathol. Pharmacol.* **1997**, *97*, 335−346.
(13) Olin, K. L.; Stearns, D. M.; Armstrong, W. H.; Keen, C. L. *Trace Elem. Electrolytes* **1994**, *11*, 182−186.
(14) Shara, M.; Yasmin, T.; Kincaid, A. E.; Limpach, A. L.; Bartz, J.; Brenneman, K. A.; Chatterjee, A.; Bagchi, M.; Stohs, S. J.; Bagchi, D. *J. Inorg. Biochem.* **2005**, *99*, 2161−2183.
(15) Shara, M.; Kincaid, A. E.; Limpach, A. L.; Sandstrom, R.; Barrett, L.; Norton, N.; Bramble, J. D.; Yasmin, T.; Tran, J.; Chatterjee, A.; Bagchi, M.; Bagchi, D. *J. Inorg. Biochem.* **2007**, *101*, 1059−1069.
(16) Evans, G. W.; Pouchnik, D. J. *J. Inorg. Biochem.* **1993**, *49*, 177−187.
(17) Rhodes, N. R.; Konovalova, T.; Liang, Q. L.; Cassady, C. J.; Vincent, J. B. *Biol. Trace Elem. Res.* **2009**, *130*, 114−130.
(18) Penner-Hahn, J. E. In *Comprehensive Coordination Chemistry II*; Elsevier: Amsterdam, 2003; *Vol. 2*, pp 159−186.

(19) (a) Aitken, J. B.; Levina, A.; Lay, P. A. *Curr. Top. Med. Chem.* **2011**, *11*, 553−571. (b) Lay, P. A.; Levina, A. In *Chemistry, Molecular Sciences and Chemical Engineering*; Reedijk, J., Ed.; Elsevier: Oxford, in press; doi 10.1016/B978-0-12-409547-2.11126-6.
(20) Levina, A.; Armstrong, R. S.; Lay, P. A. *Coord. Chem. Rev.* **2005**, *249*, 141−160.
(21) (a) Codd, R.; Levina, A.; Zhang, L.; Hambley, T. W.; Lay, P. A. *Inorg. Chem.* **2000**, *39*, 990−997. (b) Levina, A.; Zhang, L.; Lay, P. A. *Inorg. Chem.* **2003**, *42*, 767−784. (c) Levina, A.; Turner, P.; Lay, P. A. *Inorg. Chem.* **2003**, *42*, 5392−5398. (d) Cawich, C. M.; Ibrahim, A.; Link, K. L.; Bumgartner, A.; Patro, M. D.; Mahapatro, S. N.; Lay, P. A.; Levina, A.; Eaton, S. S.; Eaton, G. R. *Inorg. Chem.* **2003**, *42*, 6458−6468. (e) Levina, A.; Lay, P. A. *Inorg. Chem.* **2004**, *43*, 324−335. (f) Levina, A.; Foran, G. J.; Pattison, D. I.; Lay, P. A. *Agnew. Chem., Int. Ed. Engl.* **2004**, *43*, 462−465. (g) Levina, A.; Codd, R.; Foran, G. J.; Hambley, T. W.; Maschmeyer, T.; Masters, A. F.; Lay, P. A. *Inorg. Chem.* **2004**, *43*, 1046−1055. (h) Weeks, C. L.; Levina, A.; Dillon, C. T.; Turner, P.; Fenton, R. R.; Lay, P. A. *Inorg. Chem.* **2004**, *43*, 7844−7856. (i) Gez, S.; Luxenhofer, R.; Levina, A.; Codd, R.; Lay, P. A. *Inorg. Chem.* **2005**, *44*, 2934−2943. (j) Levina, A.; Harris, H. H.; Lay, P. A. *J. Biol. Inorg. Chem.* **2006**, *11*, 225−234. (k) Milsmann, C.; Levina, A.; Harris, H. H.; Foran, G. J.; Turner, P.; Lay, P. A. *Inorg. Chem.* **2006**, *45*, 4743−4754. (l) Levina, A.; Harris, H. H.; Lay, P. A. *J. Am. Chem. Soc.* **2007**, *129*, 1065−1075. 9832 (m) Bartholomäus, R.; Harms, K.; Levina, A.; Lay, P. A. *Inorg. Chem.* **2012**, *51*, 11238−11240. (n) Bartholomäus, R.; Irwin, J. A.; Shi, L.; Smith, S. M.; Levina, A.; Lay, P. A. *Inorg. Chem.* **2013**, *52*, 4282−4292.
(22) *WIN-EPR*, Version 921201; Bruker-Franzen Analytic: Bremen, Germany, 1992.
(23) Nguyen, A.; Mulyani, I.; Levina, A.; Lay, P. A. *Inorg. Chem.* **2008**, *47*, 4299−4309.
(24) *XFit for Windows*, beta version; Australian Synchrotron Research Program: Sydney, Australia, 2004.
(25) *FEFF*, Version 6.01; Department of Physics, University of Washington: Seattle, WA, 1992, 1993. Rehr, J. J.; Albers, R. C.; Zabinsky, S. I. *Phys. Rev. Lett.* **1992**, *69*, 3397−3400.
(26) Gabriel, C.; Raptopoulou, C. P.; Drouza, C.; Lalioti, N.; Salifoglou, A. *Polyhedron* **2009**, *28*, 3209−3220.
(27) Stearns, D. M.; Armstrong, W. H. *Inorg. Chem.* **1992**, *31*, 5178−5184.
(28) Eshel, M.; Bino, A. *Inorg. Chim. Acta* **2001**, *320*, 127−132.
(29) *Chem3D Pro*, Version 11.0.1; CambridgeSoft: Cambridge, Massachusetts, 2010.
(30) Wright, W. B.; King, G. S. D. *Acta Crystallogr.* **1953**, *6*, 305−317.
(31) Gurman, S. J. *J. Synchrotron Radiat.* **1995**, *2*, 56−63.
(32) Binsted, N.; Strange, R. W.; Hasnain, S. S. *Biochemistry* **1992**, *31*, 12117−12125.
(33) *The Unscrambler X*, Version 10.1; CAMO software AS.: Oslo, Norway, 2011.
(34) Lever, A. B. P. *J. Chem. Educ.* **1968**, *45*, 711−712.
(35) Dou, Y. *J. Chem. Educ.* **1990**, *67*, 134.
(36) Socrates, G. *Infrared and Raman characteristic group frequencies: tables and charts*, 3rd ed.; Wiley: Chichester, New York, 2001; p 366.
(37) Weckhuysen, B. M.; Schoonheydt, R. A.; Mabbs, F. E.; Collison, D. *J. Chem. Soc., Faraday Trans.* **1996**, *92*, 2431−2436.
(38) Antsyshkina, A. S.; Porai-Koshits, M. A.; Arkhangel'skii, I. V.; Diallo, I. N. *Russ. J. Inorg. Chem.* **1987**, *32*, 1700−1703.
(39) Vincent, J. B.; Bennett, R. In *The Nutritional Biochemistry of Chromium(III)*; Vincent, J. B., Ed.; Elsevier: Amsterdam, 2007; pp 139−160.
(40) Green, C. A.; Koine, N.; Legg, J. I.; Willett, R. D. *Inorg. Chim. Acta* **1990**, *176*, 87−93.
(41) Visser, H. G.; Purcell, W.; Basson, S. S. *Polyhedron* **1999**, *18*, 2795−2801.
(42) Yevitz, M.; Stanko, J. A. *J. Am. Chem. Soc.* **1971**, *93*, 1512−1513.
(43) Cline, S. J.; Glerup, J.; Hodgson, D. J.; Jensen, G. S.; Pedersen, E. *Inorg. Chem.* **1981**, *20*, 2229−2233.
(44) Andersen, P.; Hatsui, H.; Nielsen, K. M.; Nygaard, A. S. *Acta Chem. Scand.* **1994**, *48*, 542−547.
(45) Fujihara, T.; Fuyuhiro, A.; Kaizaki, S. *J. Chem. Soc., Dalton Trans.* **1995**, 1813−1821.
(46) Drljaca, A.; Hockless, D. C. R.; Moubaraki, B.; Murray, K. S.; Spiccia, L. *Inorg. Chem.* **1997**, *36*, 1988−1989.
(47) Turowski, P. N.; Bino, A.; Lippard, S. J. *Angew. Chem., Int. Ed.* **1990**, *102*, 841−842.
(48) Harton, A.; Nagi, M. K.; Glass, M. M.; Junk, P. C.; Atwood, J. L.; Vincent, J. B. *Inorg. Chim. Acta* **1994**, *217*, 171−179.
(49) Liang, S.; Liu, Z.; Liu, N.; Liu, C.; Di, X.; Zhang, J. *J. Coord. Chem.* **2010**, *63*, 3441−3452.
(50) Fujihara, T.; Fuyuhiro, A.; Kaizaki, S. *Inorg. Chim. Acta* **1998**, *278*, 15−23.
(51) Visser, H. G. *Acta Crystallogr., Sect. E: Struct. Rep. Online* **2006**, *E62*, m3272−m3274.
(52) Novitchi, G.; Costes, J.-P.; Ciornea, V.; Shova, S.; Filippova, I.; Simonov, Y. A.; Gulea, A. *Eur. J. Inorg. Chem.* **2005**, 929−937.
(53) Gispert, J. R. *Coordination Chemistry*; Wiley-VCH: New York, 2008; pp 341−376.
(54) Dunn, T. M. In *Modern Coordination Chemistry*, Lewis, J., Wilkins, R. G., Eds.; Interscience Publishers: New York, 1960; pp 229−301.